Pergamon

Int. J. Solids Structures Vol. 31, No. 14, pp. 1861–1876, 1994

0020–7683/94 \$7.00 + .00

0020–7683(94)E0024–P

BLAST LOADING OF FULLY CLAMPED CIRCULAR PLATES WITH TRANSVERSE SHEAR EFFECTS

Q. M. Li and Norman Jones
Impact Research Centre, Department of Mechanical Engineering,
The University of Liverpool, P.O. Box 147, Liverpool L69 3BX, U.K.

(*Received* 1 *September* 1993; *in revised form* 31 *January* 1994)

Abstract—The dynamic response of a fully clamped circular plate, which is made from a rigid, perfectly plastic material, is investigated with the aid of the extended Johansen yield criterion which retains the influence of the transverse shear force as well as the bending moments. Theoretical solutions are obtained for a general blast loading distributed uniformly over the entire area of a plate. The effects of different boundary conditions, pressure pulse loading shapes and the influence of the transverse shear force on the dynamic plastic response of circular plates are explored. It is found that Youngdahl's correlation parameters may be used to eliminate the effect of the pulse loading shape on the dynamic response of circular plates. The critical conditions are predicted for a transverse shear severance to occur at the supports of a circular plate (mode III failure) when transverse shear effects are retained in the yield condition. Theoretical predictions for the impulsive loading case are compared with the bound theorem predictions, which reveals that the lower bound results give good agreement with the corresponding theoretical results.

NOTATION

i_1	defined by eqn (31)
m_r, m_θ	M_r/M_0, M_θ/M_0
p	P/P_b
q	Q/Q_0
r, θ	polar coordinates defined in Fig. 1(b)
t	time
w, $\dot{w}$, $\ddot{w}$	transverse displacement, velocity and acceleration
$\bar{w}$, $\dot{\bar{w}}$, $\ddot{\bar{w}}$	dimensionless transverse displacement, velocity and acceleration defined by eqns (9d–f)
y	$[(v^2-4v+1)^{1/2}-1]/v$
$\bar{z}$	coordinate through plate thickness [Fig. 1(b)]
z	Z/R
H	circular plate thickness
I_e	effective loading parameter, defined in Youngdahl (1970) with $t_y = 0$
I_0	loading impulse per unit area
I_1	defined by eqn (30a)
I_r	rotatory inertia per unit length
M_r, M_θ	radial and circumferential bending moments per unit length as defined in Fig. 1(b)
M_0	magnitude of bending moment per unit length required for the plastic flow of a circular plate cross-section
P_b	static plastic bending collapse pressure for a fully clamped or a simply supported circular plate
P_e	effective loading parameter, defined in Youngdahl (1970) with $t_y = 0$
P_0	$12\,M_0/R^2$
P_1	defined by eqn (30b)
$P(t)$	pressure loading
Q	transverse shear force per unit length of a circular plate [Fig. 1(b)]
Q_0	magnitude of Q required for plastic flow of a circular plate cross-section
R	radius of a circular plate
W_0, W_1	transverse displacements at the mid-point and supports of a circular plate, respectively
$\bar{W}_0$, $\bar{W}_1$	dimensionless values of W_0 and W_1 defined by $\bar{W}_i = W_i/(I_0^2/\mu P_b)$, $i = 0, 1$
W_0^*, W_1^*	dimensionless values of W_0 and W_1 defined by $W_i^* = W_i/(I_0^2/\mu P_0)$, $i = 0, 1$
Z	location of the interface defined in Fig. 4
μ	ρH
v	$Q_0R/2M_0$
ξ	r/R
ρ	density of material
τ	$t/(I_0/P_b)$
$(\dot{\ })$	$\partial(\ )/\partial t$ or $\partial(\ )/\partial\tau$.

1. INTRODUCTION

A theoretical investigation was reported recently by Li and Jones (1991a) on the dynamic plastic response of a fully clamped beam with the influence of the transverse shear force retained in the yield condition. It transpires from a comparison with the theoretical solution for a simply supported beam [see e.g. Nonaka (1977)] that the boundary conditions exercise a strong influence on the dynamic plastic response of beams. The present paper presents a theoretical solution for the dynamic plastic response of a fully clamped circular plate and compares it with the corresponding simply supported case.

It is observed that fewer studies have been reported on fully clamped circular plates than on simply supported circular plates mainly because of the difficulties in constructing flow fields which are both kinematically and statically admissible for a rigid, perfectly plastic material. Wang and Hopkins (1954) published the first theoretical solution for a fully clamped circular plate when subjected to an impulsive pressure loading and with plastic yielding controlled by the Tresca yield criterion. This work was extended by Florence to cater for a rectangular pressure pulse [see e.g. Florence (1966a)] and for a central blast loading [see e.g. Florence (1966b)]. Florence (1977) also obtained theoretical solutions for a circular plate subjected to a central rectangular pressure pulse loading and with plastic yielding controlled by the Johansen yield criterion. Hopkins (1957) compared the predictions for the dynamic plastic response of both simply supported and fully clamped circular plates with plastic yielding controlled by the Tresca and Johansen yield criteria. However, the influence of the transverse shear force on plastic yielding was not examined in any of the above studies.

The dynamic plastic response of simply supported circular plates was examined by Jones and Gomes de Oliveira (1980). This study confirmed the importance of transverse shear forces for small values of the dimensionless parameter $v = Q_0R/2M_0$. Kumar and Krishna Reddy (1986) presented a theoretical solution for a rectangular pressure pulse loading, which was extended by Li and Huang (1990) and Li and Jones (1991b) to a general blast pressure loading. The yield criterion proposed by Sawczuk and Duszek (1963), which is an extension of the Tresca yield criterion, was used for the behaviour of the plate material in all of the above analyses. It has been shown that theoretical solutions for the dynamic plastic response of simply supported circular plates subjected to a blast pressure loading are the same for both the extended Johansen and the extended Tresca yield criteria [see e.g. Li and Jones (1991b)].

In the present work, the dynamic plastic response of a fully clamped circular plate, made from a rigid, perfectly plastic material, is investigated. Theoretical solutions for a general blast loading distributed uniformly over the entire plate were obtained with the aid of the extended Johansen yield criterion, which retains the transverse shear force in addition to the bending moments. The effects of different boundary conditions and the influence of the transverse shear force as well as the pulse loading shape effects and the use of a bound theorem are discussed in Section 4.

2. GENERAL EQUATIONS

The equilibrium equations for the circular plate element shown in Fig. 1 may be written in the form

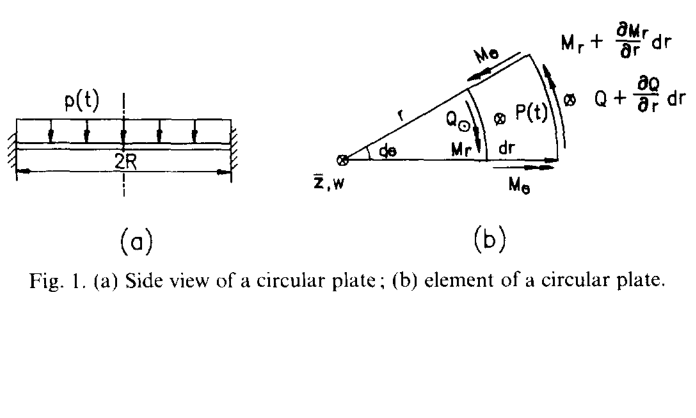

Fig. 1. (a) Side view of a circular plate; (b) element of a circular plate.

$$\frac{\partial M_r}{\partial r}+\frac{(M_r-M_\theta)}{r}+Q=0 \tag{1a}$$

and

$$\frac{\partial Q}{\partial r}+\frac{Q}{r}=-P(t)+\mu\frac{\partial^2 w}{\partial t^2} \tag{1b}$$

when neglecting rotatory inertia, and where $\mu=\rho H$, $\partial w/\partial r=\psi+\gamma$, ψ is the rotation of a line originally perpendicular to the initial mid-plane due to bending, and $\gamma=\partial w/\partial r-\psi$, $\kappa_r=\partial\psi/\partial r$ and $\kappa_\theta=\psi/r$ are the transverse shear strain, radial curvature change and circumferential curvature change, respectively.

The extended Johansen yield criterion (Fig. 2) is used in the following analysis. Generally speaking, the Johansen and Tresca yield criteria are used to describe the properties of reinforced concrete and metal plates, respectively. However, the size of the Johansen yield criterion may be adjusted to circumscribe or inscribe the exact yield curve to provide approximate bounds for a theoretical solution.

The dynamic continuity conditions across a discontinuity front may be written as [see e.g. Jones and Gomes de Oliveira (1980)]

$$[M_r]=-\dot{Z}I_r[\dot{\psi}] \tag{2a}$$

and

$$[Q]=-\dot{Z}\mu[\dot{w}], \tag{2b}$$

where $[A]=A_2-A_1$ is the difference of the quantity A across a discontinuity interface.

Continuity of the transverse displacement and of the angular deformation associated with the radial bending of a circular plate requires

$$[\psi]=0 \quad \text{and} \quad [w]=0$$

across the interface, which lead to [see e.g. Jones and Gomes de Oliveira (1980)]

$$[\dot{\psi}]=-\dot{Z}\left[\frac{\partial\psi}{\partial r}\right] \tag{3a}$$

and

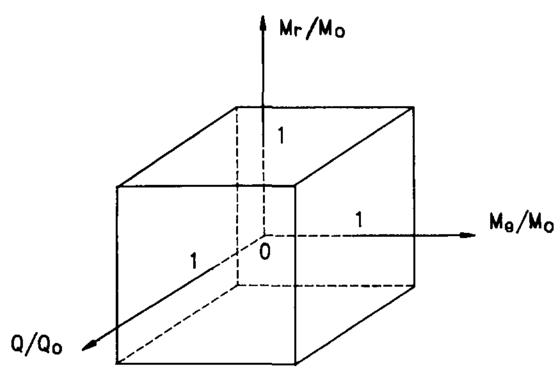

Fig. 2. Extended Johansen yield surface.

$$[\dot{w}] = -\dot{Z}\left[\frac{\partial w}{\partial r}\right]. \tag{3b}$$

Similar theoretical procedures to those in Jones (1989) for a beam lead to the following classification of the continuity conditions for an axisymmetrically loaded circular plate with $I_r = 0$:

(a) conditions at a travelling circular bending hinge

$$[M_r] = 0, \quad [Q] = 0, \quad [\dot{w}] = 0, \quad [w] = 0; \tag{4a–d}$$

(b) conditions at a stationary circular bending hinge

$$[M_r] = 0, \quad [Q] = 0, \quad [\dot{w}] = 0, \tag{5a–c}$$

in which $[\dot{w}] = 0$ is equivalent to $[w] = 0$;

(c) conditions at a stationary interface with both a bending hinge and a transverse shear slide

$$[M_r] = 0, \quad [Q] = 0. \tag{6a,b}$$

All these conditions satisfy the conservation of angular and linear momenta [eqn (2a) with $I_r = 0$ and eqn (2b)] and the corresponding kinematical continuity conditions.

The simplified case of a blast loading, shown in Fig. 3, is examined in the following sections when it is distributed uniformly over the entire area of a plate.

Equations (1a,b) and the continuity conditions across a circular bending hinge can be expressed in the dimensionless forms

$$\frac{\partial(m_r \xi)}{\partial \xi} - m_\theta + 2vq\xi = 0, \tag{7a}$$

$$\frac{\partial(q\xi)}{\partial \xi} = \frac{6(\ddot{w}-p)\xi}{v} \tag{7b}$$

and

$$[m_r] = 0, \quad [q] = 0, \quad [\dot{\bar{w}}] = 0, \quad [\bar{w}] = 0, \tag{8a–d}$$

respectively, where

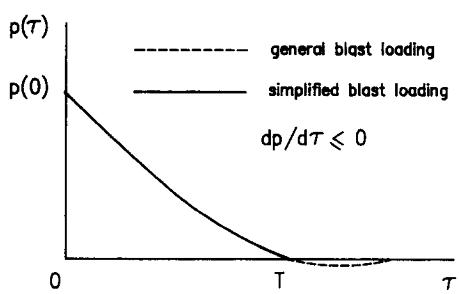

Fig. 3. Blast loading.

$$m_r = \frac{M_r}{M_0},\quad m_\theta = \frac{M_\theta}{M_0},\quad q = \frac{Q}{Q_0},\quad \bar{w} = \frac{w}{I_0^2/\mu P_b},\quad \dot{\bar{w}} = \frac{\dot{w}}{I_0^2/\mu},\quad \ddot{\bar{w}} = \frac{\ddot{w}}{P_b/\mu},$$

$$\xi = \frac{r}{R},\quad \tau = \frac{t}{I_0/P_b},\quad p = \frac{P}{P_b},\quad v = \frac{Q_0 R}{2M_0},\quad z = \frac{Z}{R} \tag{9a–k}$$

and I_0 is the loading impulse per unit area. A static plastic bending collapse pressure of $P_b = 12\,M_0/R^2$ is used in eqns (9a–k) for a fully clamped circular plate with yielding controlled by the Johansen yield criterion [see e.g. Florence (1977)]. The collapse pressure corresponding to the Tresca yield criterion is 6.6% smaller, or $P_b = 11.26\,M_0/R^2$ [see e.g. Hopkins and Prager (1953) and Jones (1989)].

3. THEORETICAL SOLUTIONS FOR BLAST LOADING

The forms of the initial transverse velocity profiles for fully clamped circular plates depend on both the parameter v and the initial intensity of the external loading, as indicated in Fig. 4 and shown in the following section.

3.1. *Class I plates*, $0 < v \leqslant 3$ [*case* (*a*) *in Fig.* 4]

The transverse velocity profile is uniform over the entire plate, as indicated in Fig. 4. Thus, substituting a uniform profile into eqns (7a,b), and using $q = -1$ and $m_r = 1$ at $\xi = 1$ as well as $m_\theta = \text{const}$ for $0 \leqslant \xi \leqslant 1$ gives

$$\dot{\bar{w}} = \int_0^\tau p\,\mathrm{d}\tau - v\frac{\tau}{3}. \tag{10}$$

Differentiating eqn (10) with respect to time and putting $\ddot{\bar{w}} = 0$ gives $P = P_b v/3 = 2Q_0/R$, which is the static plastic collapse pressure required to cause transverse shear sliding around the supports of a circular plate. The final transverse displacement profile may be obtained by integrating eqn (10). It is straightforward to show that the dimensionless response time is

$$\tau_f = 3\frac{\int_0^{\tau_f} p\,\mathrm{d}\tau}{v}, \tag{11}$$

while the associated transverse shear force and bending moments are

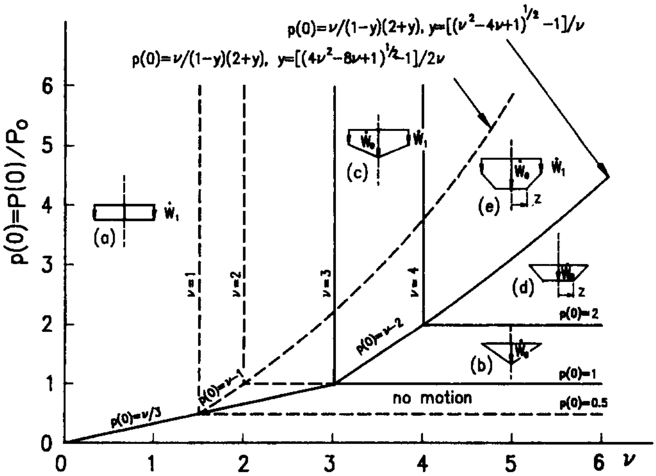

Fig. 4. Initial transverse velocity profiles: ——: fully clamped circular plate; – – –: simply supported circular plate [see e.g. Li and Huang (1990)].

$$q = -\xi, \quad m_\theta = 1 - \frac{2v}{3} \quad \text{and} \quad m_r = 1 - \frac{2v(1-\xi^2)}{3}, \tag{12a–c}$$

respectively. It may be shown that $-1 \leqslant q \leqslant 0$, $-1 \leqslant m_\theta < 1$ and $-1 \leqslant m_r \leqslant 1$ for $0 \leqslant \tau \leqslant \tau_f$ and $0 \leqslant \xi \leqslant 1$ when $0 < v \leqslant 3$.

3.2. *Class II plates*, $3 < v \leqslant 4$

There are two different cases in this class of plates which depend on the value of the parameter v and the initial magnitude of the external dynamic loading, as shown in Fig. 4. Transverse shear sliding develops at the supports, in one case, but not in the other.

3.2.1. $1 \leqslant p(0) \leqslant v-2$ [*case (b) in Fig.* 4]. No transverse sliding occurs at the supports of a circular plate in this case. The transverse velocity field is linear as indicated in Fig. 4 for case (b), which, when substituting into eqns (7a,b) and using $q = 0$ and $m_r = m_\theta$ at $\xi = 0$, $m_r = 1$ at $\xi = 1$ and $m_\theta = -1$ for $0 \leqslant \xi \leqslant 1$, gives

$$\dot{w} = 2\left[\int_0^\tau p\,\mathrm{d}\tau - \tau\right](1-\xi). \tag{13}$$

It should be noted that if $\ddot{w} = 0$ in the derivation of eqn (13), then the static bending collapse pressure for a fully clamped circular plate, $P_b = 12\,M_0/R^2$, is recovered.

The associated dimensionless transverse shear force and bending moments are

$$q = \frac{3(p-2)\xi}{v} - \frac{4(p-1)\xi^2}{v}, \quad m_\theta = -1 \quad \text{and} \quad m_r = -1-2(p-2)\xi^2+2(p-1)\xi^3, \tag{14a–c}$$

respectively, and $p(0) \leqslant v-2$ in order to avoid $q \geqslant -1$ at $\xi = 1$.

Motion ceases when

$$\tau_f = \int_0^{\tau_f} p\,\mathrm{d}\tau \tag{15}$$

which requires $p(0) \geqslant 1$ for the existence of the solution.

3.2.2. $p(0) > v-2$. There are two phases of motion in this case:

(a) first phase of motion, $0 \leqslant \tau \leqslant \tau_1$ [case (c) in Fig. 4]

Transverse shear displacements develop around the supports of a fully clamped circular plate, as indicated by the transverse velocity profile for case (c) in Fig. 4. Now substituting this velocity profile into eqns (7a,b) gives

$$\dot{w} = \int_0^\tau p\,\mathrm{d}\tau + (2-v)\tau + 2(v-3)\tau(1-\xi) \tag{16}$$

when satisfying the requirements $q = 0$ and $m_r = m_\theta$ at $\xi = 0$, $m_r = 1$ and $q = -1$ at $\xi = 1$ and $m_\theta = -1$ for $0 \leqslant \xi \leqslant 1$. The associated generalized stresses are

$$q = \frac{[3(v-4)-4(v-3)\xi]\xi}{v}, \quad m_\theta = -1 \tag{17a,b}$$

and

$$m_r = -1-2[\nu-4-(\nu-3)\xi]\xi^2, \tag{17c}$$

which, for $\partial^2 m_r/\partial\xi^2 \geqslant 0$ at $\xi = 0$, requires $\nu \leqslant 4$ in order to avoid a yield violation. The dimensionless time τ_1, when the transverse shear displacements cease at the supports, is determined from the condition $\bar{w} = 0$ at $\xi = 1$ (i.e. $\bar{W}_1 = 0$), or

$$\tau_1 = \frac{\int_0^{\tau_1} p\,\mathrm{d}\tau}{\nu-2}. \tag{18}$$

(b) second phase of motion, $\tau_1 < \tau \leqslant \tau_f$ [case (b) in Fig. 4]

The theoretical solution for this phase of motion is similar to that in Section 3.2.1 with the initial conditions evaluated at the end of the first phase of motion.

3.3. *Class III plates*, $\nu > 4$

It turns out that there are three different cases associated with various values of $p(0)$ for this class of plates. However, the theoretical solution is the same as that in Section 3.2.1 when $p(0) < 2$, so that the subsequent analyses are developed only for the inequality $p(0) \geqslant 2$.

3.3.1. $2 \leqslant p(0) \leqslant \nu/(1-y)(2+y)$, $y = [(\nu^2-4\nu+1)^{1/2}-1]/\nu$. No transverse shear sliding occurs at the supports of a fully clamped plate in this case but the response consists of two phases of motion:

(a) first phase of motion, $0 \leqslant \tau \leqslant \tau_1$ [case (d) in Fig. 4]

The dimensionless transverse velocity field for this case is

$$\dot{\bar{w}} = \dot{\bar{W}}_0, \quad 0 \leqslant \xi \leqslant z \tag{19a}$$

and

$$\dot{\bar{w}} = \frac{\dot{\bar{W}}_0(1-\xi)}{1-z}, \quad z \leqslant \xi \leqslant 1. \tag{19b}$$

Substituting eqn (19a) into eqns (7a,b), together with the requirements of $q = 0$ and $m_r = m_\theta = -1$ in $0 \leqslant \xi \leqslant z$, leads to

$$\dot{\bar{W}}_0 = \int_0^{\tau} p\,\mathrm{d}\tau. \tag{20}$$

The generalized stresses in the outer annular region $z < \xi \leqslant 1$ may be derived by integrating eqns (7a,b) after substituting eqn (19b) and using the continuity conditions as well as $m_\theta = -1$

$$q = \frac{3\left[p(1-z)-p(1-z)^2+\dot{z}\int_0^{\tau} p\,\mathrm{d}\tau\right](\xi^2-z^2)}{\nu(1-z)^2\xi} - \frac{2\left[p(1-z)+\dot{z}\int_0^{\tau} p\,\mathrm{d}\tau\right](\xi^3-z^3)}{\nu(1-z)^2\xi}, \tag{21a}$$

$$m_\theta = -1 \tag{21b}$$

and

$$m_r = -1 - \frac{2\left[p(1-z)-p(1-z)^2+\dot{z}\int_0^\tau p\,\mathrm{d}\tau\right](\xi-z)^2(\xi+2z)}{(1-z)^2\xi} + \frac{\left[p(1-z)+\dot{z}\int_0^\tau p\,\mathrm{d}\tau\right](\xi-z)^2(\xi^2+2z\xi+3z^2)}{(1-z)^2\xi}, \quad (21c)$$

where z is a function of the dimensionless time τ, which is determined from $m_r = 1$ at $\xi = 1$, or

$$z^3-z^2-z+1 = \frac{2\tau}{\int_0^\tau p\,\mathrm{d}\tau}. \quad (22)$$

Now, $z(\tau_1) = 0$ when the travelling plastic hinge reaches the mid-span, or

$$\tau_1 = \frac{\int_0^{\tau_1} p\,\mathrm{d}\tau}{2}. \quad (23)$$

The initial position of the hinge in a circular plate is obtained from eqn (22)

$$z_0^3-z_0^2-z_0+1 = \frac{2}{p(0)}, \quad (24)$$

when using

$$\lim|_{\tau\to 0}\left(2\tau\Big/\int_0^\tau p\,\mathrm{d}\tau\right) = \frac{2}{p(0)}.$$

It should be noted that the requirement $q = -1$ at $\xi = 1$ when $\tau = 0$ from eqn (21a) leads to $p(0) = v/(2-y-y^2)$, where $y = [(v^2-4v+1)^{1/2}-1]/v$. Therefore, $p(0) \leqslant v/(1-y)(2+y)$ should be satisfied in this case in order that $q \geqslant -1$ at $\xi = 1$ when $\tau = 0$; otherwise, the results are given in Section 3.3.2.

(b) second phase of motion, $\tau_1 < \tau \leqslant \tau_f$ [case (b) in Fig. 4]

The solution for this phase of motion is similar to that examined previously in Section 3.2.1 except for the initial conditions which may be obtained from the end of the first phase of motion.

3.3.2. $p(0) > v/(1-y)(2+y)$. There are three phases of motion in this particular case, with transverse shear sliding occurring at the supports only during the first phase of motion:

(a) first phase at motion, $0 \leqslant \tau \leqslant \tau_1$ [case (e) in Fig. 4]

In this phase of motion, transverse shear sliding develops around the supports of a fully clamped plate and the circular plastic hinges remain stationary. By using procedures similar to those outlined earlier, the dimensionless transverse velocity field may be written in the form

$$\dot{w} = \int_0^\tau p\,\mathrm{d}\tau, \quad 0 \leqslant \xi \leqslant z \quad (25a)$$

and

$$\dot{w} = \int_0^\tau p\,\mathrm{d}\tau - \frac{v\tau(\xi - z)}{(2-z-z^2)(1-z)}, \quad z < \xi \leqslant 1, \tag{25b}$$

where $z = y = [(v^2-4v+1)^{1/2}-1]/v$.

The requirement that $\dot{w} = 0$ at $\xi = 1$ (i.e., $\dot{W}_1 = 0$) at the end of this phase of motion occurs when

$$\tau_1 = \frac{(2-y-y^2)\int_0^{\tau_1} p\,\mathrm{d}\tau}{v}. \tag{26}$$

It may be shown that the dimensionless transverse shear force and bending moments are

$$q = 0, \quad 0 \leqslant \xi \leqslant y, \tag{27a}$$

$$q = \frac{3y(\xi^2-y^2)-2(\xi^3-y^3)}{\xi(1-y)(2-y-y^2)}, \quad y < \xi \leqslant 1, \tag{27b}$$

$$m_\theta = -1, \quad 0 \leqslant \xi \leqslant 1, \tag{28}$$

$$m_r = -1, \quad 0 \leqslant \xi \leqslant y \tag{29a}$$

and

$$m_r = -1 + \frac{v(\xi+y)(\xi-y)^3}{\xi(1-y)^2(2+y)}, \quad y < \xi \leqslant 1, \tag{29b}$$

respectively.

(b) second phase of motion, $\tau_1 < \tau \leqslant \tau_2$ [case (d) in Fig. 4]

The results for this phase of motion are similar to those for the first phase in Section 3.3.1 except that the initial conditions are obtained from the end of the first phase of motion in Section 3.3.2(a). It transpires that τ_2 is determined from eqn (23).

(c) third phase of motion, $\tau_2 < \tau \leqslant \tau_f$ [case (b) in Fig. 4]

The results for this phase of motion are similar to those in Section 3.2.1 when allowing for the different initial conditions.

The theoretical results obtained for all of the above cases are shown to be statically admissible in Section 4. Therefore, these theoretical solutions are both statically and kinematically admissible, and are exact theoretical solutions for the problem posed in Section 2 when plastic yielding is controlled by the yield condition in Fig. 2.

4. DISCUSSION

It is interesting to compare the present theoretical results for the blast loading of a fully clamped rigid, perfectly plastic circular plate with the theoretical predictions for a simply supported circular plate published previously in Li and Huang (1990) and Li and Jones (1991b). It transpires that when replacing the dimensionless parameter v in the present paper for a fully clamped circular plate by $2v$, then the results are exactly the same as the corresponding values for a blast loaded simply supported circular plate, except for the bending moments. However, the bending moments, m_θ^c and m_r^c, for a fully clamped circular plate, may be expressed in the form $m_\theta^c = 1+2m_\theta^s$ and $m_r^c = 1+2m_r^s$, respectively, where m_θ^s and m_r^s are the bending moments for a simply supported circular plate [see e.g. Li and Jones (1991b)]. Similar relationships have been obtained recently for fully clamped and simply supported beams subjected to blast loads [see e.g. Li and Jones (1991a)]. It appears for both beams and circular plates that the theoretical rigid–plastic predictions may be evaluated for one boundary condition and used for the other by a simple substitution of the parameter ν. It is important to note that these relationships exist only for the simplified square or cubic yield criterion because it has been shown that the dynamic plastic response of a fully clamped circular plate controlled by the Tresca yield criterion [see e.g. Florence (1966b)] is different from that controlled by the Johansen yield criterion [see e.g. Florence (1977)]. Therefore, the difference between the extended Tresca and the extended Johansen yield criteria will lead to different dynamic plastic responses of a fully clamped circular plate under blast loading conditions. However, the dynamic plastic response of a simply supported circular plate has the same form for both the extended Tresca and extended Johansen yield criteria, because the locus of the generalized stresses on the extended Tresca yield surface is also on the extended Johansen yield surface [see e.g. Li and Jones (1991b)].

Li and Jones (1991b) have proved the static admissibility of the generalized stresses for a simply supported circular plate, which requires that q^s, m_θ^s and m_r^s satisfy inequalities $-1 \leqslant q^s \leqslant 1$, $-1 \leqslant m_\theta^s \leqslant 1$ and $-1 \leqslant m_r^s \leqslant 1$ on the plate during the plastic response period. According to the relationships between the theoretical results for simply supported and fully clamped circular plates presented above, it is straightforward to reach the same conclusions for a fully clamped circular plate, i.e. $-1 \leqslant q^c \leqslant 1$, $-1 \leqslant m_\theta^c \leqslant 1$ and $-1 \leqslant m_r^c \leqslant 1$. Thus, the generalized stresses in the present paper are statically admissible.

Figure 4 shows the regions of validity for the initial transverse velocity profiles of both fully clamped and simply supported circular plates. For a given value of ν, transverse shear sliding develops more easily in a fully clamped circular plate than in a similar simply supported circular plate. Therefore, a simply supported circular plate has a greater capacity to resist transverse shear forces than a fully clamped circular plate.

The variation of the dimensionless transverse shear forces and bending moments with ξ are shown in Fig. 5 for the transverse shear sliding phases of simply supported and fully clamped circular plates. Similar to the observations for beams [see Fig. 5 in Li and Jones (1991a)], the magnitude of the transverse shear force is important throughout a greater area of a fully clamped circular plate.

When $\nu > 4$ for a fully clamped circular plate (or $\nu > 2$ for a simply supported circular plate), a circular plastic bending hinge develops between the mid-point and supports of a circular plate, as shown in Fig. 4 for cases (d) and (e) with travelling and stationary circular plastic hinges, respectively. It is evident from Fig. 6(a) that the initial radial position of a travelling circular plastic hinge increases with the initial intensity of the external loading, while the radial position of a stationary circular plastic hinge is greater for larger values of the parameter ν [Fig. 6(b)]. In both cases, the initial radial position of a circular plastic hinge in a simply supported circular plate is closer to the supports than in a fully clamped circular plate.

It is evident from Fig. 7 that the permanent central transverse displacement, W_0^*, for a simply supported circular plate is larger than that for a similar fully clamped circular plate. In fact, it is about 2.46 times larger for $\nu > 4$ when $p = 2.1$, as shown in Fig. 7.

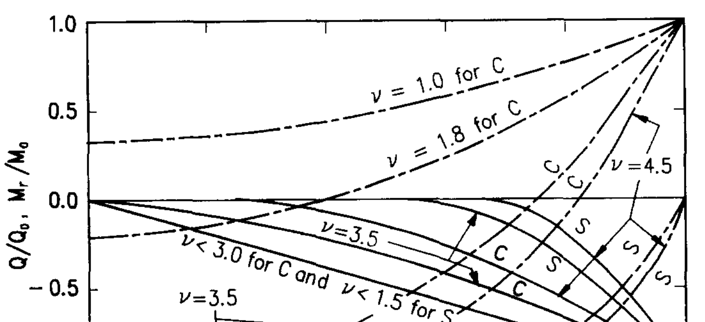

Fig. 5. Variations of the dimensionless transverse shear force and the dimensionless radial bending moment with ξ during the transverse shear sliding phase: C: fully clamped circular plate; S: simply supported circular plate; ——: q; - — -: m_r.

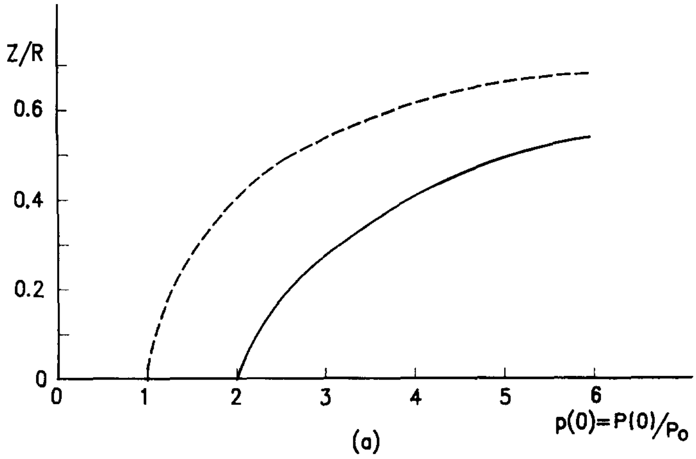

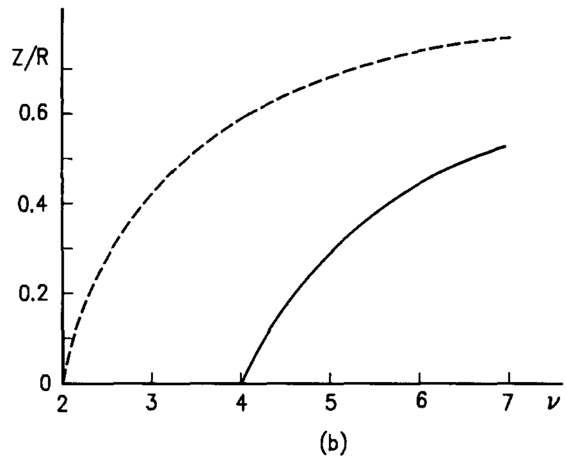

Fig. 6. (a) Initial position of the bending hinge for case (d) in Fig. 4; (b) initial position of the bending hinge during the transverse sliding phase [case (e) in Fig. 4]; ——: fully clamped case; ---: simply supported case.

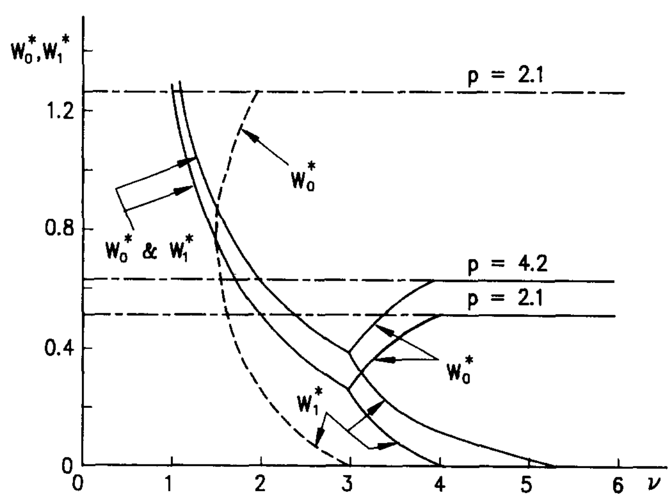

Fig. 7. Variations of the dimensionless central and edge displacements with the parameter ν for a rectangular pressure loading: ——: fully clamped case; ---: simply supported case; -·-: bending only solutions, where $p = P/P_0$.

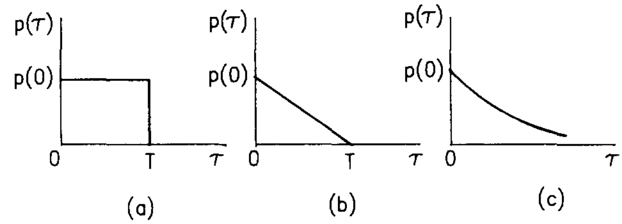

Fig. 8. Pressure–time histories: (a) rectangular shaped pressure loading; (b) linearly decreasing pressure loading; (c) exponentially decreasing pressure loading.

However, the permanent transverse shear sliding at the supports of a simply supported circular plate, W_1^*, is smaller than that for a similar fully clamped plate when $v > 1.5$, as shown in Fig. 7. Thus, the boundary restraint enhances the bending capability of a fully clamped circular plate at the expense of a lower transverse shear sliding resistance at the supports. This leads to an interesting design problem which has not been noted previously.

It has been shown by Youngdahl (1970, 1971) that differences in the shapes of the external pressure pulse may have a significant effect on the dynamic plastic response of circular plates. Youngdahl introduced correlation parameters to eliminate the loading shape effects on the bending only solutions for circular plates [see e.g. Youngdahl (1970) and Jones (1989)]. These correlation or effective loading parameters are also used in the present paper in order to eliminate the effects of different loading shapes when the influence of transverse shear forces is retained in the yield criterion. Three particular pulse shapes, shown in Fig. 8, are examined in the present paper. The theoretical predictions for the dimensionless final displacements at the mid-point of a fully clamped circular plate are nearly independent of the pulse shape (Fig. 9) when the effective loading parameters I_e and P_e with $t_y = 0$ are introduced [see e.g. Youngdahl (1970)]. Thus, it is evident that the effective loading parameters are also valuable for examining the dynamic plastic response of circular plates when the influence of the transverse shear force is retained in the yield criterion.

When the magnitude of the initial loading lies within the regions labelled (a), (c) and (e) in Fig. 4, then transverse shear sliding develops at the supports of a fully clamped circular plate, which, for sufficiently severe loadings, may lead to transverse shear severance at the supports, as observed previously for beams [see e.g. Jones (1976)]. The influence of the shape of the loading pulse on the severance of a fully clamped beam is discussed by Li and Jones (1991a) for blast loadings causing large transverse shear forces. These effects are

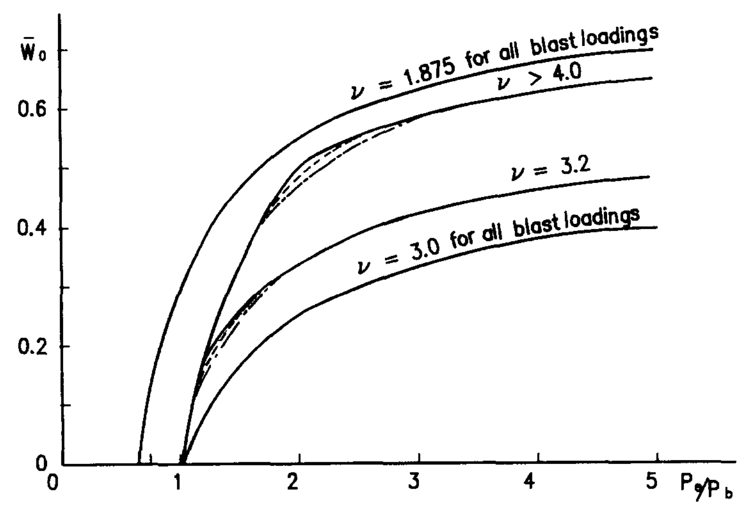

Fig. 9. Effects of the pulse shape on the maximum dimensionless final displacement at the mid-point: ——: loading case (a) in Fig. 8; – – –: loading case (b); –·–·–: loading case (c) and $I_e = \int_0^{t_f} P(t)\,dt$, $P_e = I_e^2/2\int_0^{t_f} tP(t)\,dt$, t_f is the response duration.

also significant for the fully clamped circular plates which are examined in the present paper. However, such effects may be eliminated by modifying the correlation parameters which were used to obtain the results in Fig. 9 and are defined here by

$$I_1 = \int_0^{t_1} P(t)\,\mathrm{d}t \tag{30a}$$

and

$$P_1 = \frac{I_1^2}{2\int_0^{t_1} tP(t)\,\mathrm{d}t}, \tag{30b}$$

where t_1 is the response time of the transverse shear sliding phase.

Now, the transverse velocity distributions in Section 3 for the transverse sliding phases [eqns (10, 11), (16, 18) and (25b, 26)] predict

$$i_1^2\left(\frac{1}{f(v)} - \frac{1}{p_1}\right) = 2, \tag{31}$$

where

$$f(v) = \frac{v}{3}, \qquad 0 < v \leqslant 3,$$

$$f(v) = v-2, \qquad 3 < v \leqslant 4,$$

$$f(v) = \frac{v}{2-y-y^2}, \quad v > 4, \tag{32a–c}$$

$y = [(v^2-4v+1)^{1/2}-1]/v$, $i_1 = I_1/\sqrt{\alpha\mu HP_b}$, $p_1 = P_1/P_b$, and $\alpha H (0 < \alpha \leqslant 1)$ is the critical thickness for the transverse shear failure around the boundary of a fully clamped circular plate. Jouri and Jones (1988) reported an experimental study into the values of the parameter α associated with the dynamic failure of fully clamped double-shear beams. However, no similar studies appear to have been published for a fully clamped circular plate, although some recent experimental results have been reported by Teeling-Smith and Nurick (1991) and Nurick and Teeling-Smith (1992) on the mode I–III failures of fully clamped circular plates. Thus, further experimental tests are required in order to determine the values of α for fully clamped circular plates. Equation (31) is plotted in Fig. 10 for several values of

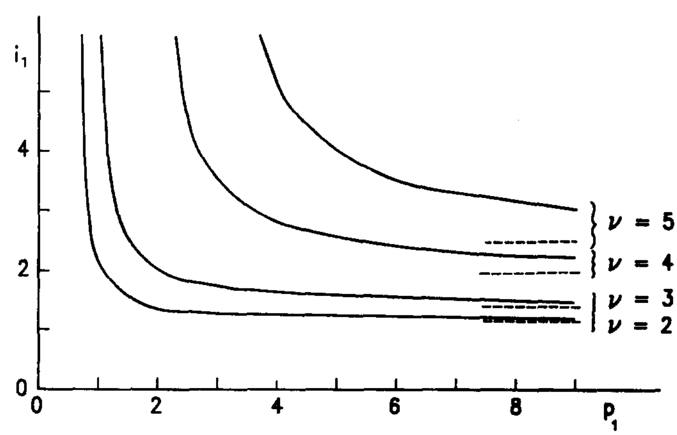

Fig. 10. Critical curves according to eqn (31) for the severance around the supports of a fully clamped circular plate: ---: value of i_1 when $p_1 \to \infty$.

Table 1. Final displacements at the mid-point and supports for a rectangular pressure loading

Class I	$0 < v \leqslant 3$	
$p \leqslant v/3$	$\bar{w}_{0f} = \bar{w}_{1f} = 0$	
$p > v/3$	$\bar{w}_{0f} = \bar{w}_{1f} = 3/2v - 1/2p$	$\tau_f = \tau_s = 3/v$
Class II	$3 < v \leqslant 4$	
$p \leqslant 1$	$\bar{w}_{0f} = \bar{w}_{1f} = 0$	
$1 < p \leqslant v-2$	$\bar{w}_{0f} = 1 - 1/p, \quad \bar{w}_{1f} = 0$	$\tau_f = 1, \quad \tau_s = 0$
$p > v-2$	$\bar{w}_{0f} = 1 - 1/2p - 1/2(v-2)$ $\bar{w}_{1f} = 1/2(v-2) - 1/2p$	$\tau_f = 1$ $\tau_s = 1/(v-2)$
Class III	$v > 4(y = [(v^2 - 4v + 1)^{1/2} - 1]/v, \quad A = (1-y)(2+y))$	
$p \leqslant 2$	same as the results for $1 < p \leqslant v-2$ in Class II	
$2 < p \leqslant v/A$	$\bar{w}_{0f} = 3/4 - 1/2p, \quad \bar{w}_{1f} = 0$	$\tau_f = 1, \quad \tau_s = 0$
$p > v/A$	$\bar{w}_{0f} = 3/4 - 1/2p$ $\bar{w}_{1f} = A/2v - 1/2p$	$\tau_f = 1$ $\tau_s = A/v$

the parameter v to give the critical curves for the transverse shear severance around the supports of a fully clamped circular plate. These critical curves, which incorporate Youngdahl's correlation parameters, may be used for any of the blast loadings in Fig. 8 and any others having a peak value at $t = 0$ and $\dot{p}(t) \leqslant 0$. Figure 10 also reveals that v is an important parameter in assessing the capability of a circular plate to resist a transverse shear failure around the supports.

For the convenience of a reader, Table 1 summarizes the theoretical predictions from the present analysis for the transverse dimensionless final displacements at the mid-point ($\bar{w}_{0f}$) and supports ($\bar{w}_{1f}$) of circular plates when subjected to a rectangular shaped pressure–time history, where $\bar{w}_{if} = w_{if}/(\mu V_0^2/P_b)$, $i = 0, 1$; τ_s is the response period for transverse shear sliding phase.

Theoretical predictions of the transverse displacement at the mid-point of a fully clamped circular plate subjected to a uniformly distributed impulsive loading (V_0) are given by integrating the corresponding transverse velocity distributions in Section 3 (or by using the corresponding results in Table 1) with $I_0 = \mu V_0$, $p(0) \to \infty$ and $\int_0^\tau p \, d\tau = 1$ for $\tau > 0$. Thus,

$$\bar{w}_{0f} = \frac{3}{2v}, \quad 0 < v \leqslant 3, \tag{33a}$$

$$\bar{w}_{0f} = \frac{2v-5}{2(v-2)}, \quad 3 < v \leqslant 4 \tag{33b}$$

and

$$\bar{w}_{0f} = \frac{3}{4}, \quad v > 4. \tag{33c}$$

It is evident that eqn (33c) is independent of v and is, therefore, identical to the bending only solution for a uniformly distributed impulsive velocity which is a special case of the theoretical results for a central rectangular pressure loading obtained by Florence (1977) using the Johansen yield condition.

The predictions of the upper [see e.g. Martin (1964)] and lower [see e.g. Morales and Nevill (1970)] bound theorems for an impulsively loaded rigid, perfectly plastic continuum are discussed in Jones (1985) and Li and Jones (1991a) when the influence of transverse shear effects are retained in the equations which govern the behaviour of structural members. These theorems for the present problem give

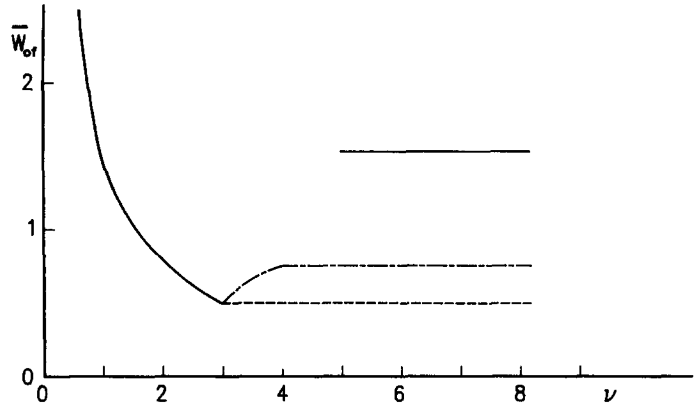

Fig. 11. Dimensionless maximum transverse displacements for an impulsively loaded fully clamped circular plate: ——: upper bound; – – –: lower bound; - — -: theoretical results predicted by eqns (33a–c) in the present paper.

$$\frac{3}{2\nu} \leqslant \bar{w}_{0f} \leqslant \frac{3}{2\nu}, \quad \text{for} \quad 0 < \nu \leqslant 3, \tag{34a}$$

$$\bar{w}_{0f} \geqslant \frac{1}{2}, \quad \text{for} \quad \nu > 3 \tag{34b}$$

and

$$\frac{1}{2} < \bar{w}_{0f} \leqslant \frac{3}{2}, \quad \text{for} \quad \nu \to \infty. \tag{34c}$$

Comparisons are made in Fig. 11 between these bound estimates and the predictions of the present theoretical method [eqns (33a–c)]. It is evident that eqn (34a) is identical to eqn (33a) for $0 < \nu \leqslant 3$, and that the lower bound from inequality (34b) is close to the theoretical values given by eqn (33b,c) for $\nu > 3$. However, there is no strictly valid upper bound for $\nu > 3$, except for $\nu \to \infty$, as discussed by Jones (1985).

In the present analysis, rotatory inertia effects are neglected in the equilibrium equations and in the continuity relations. The influence of rotatory inertia on the dynamic plastic response of simply supported circular plates has been discussed by Jones and Gomes de Oliveira (1980) and Li and Huang (1989), which conclude that the simpler theoretical analyses which neglect rotatory inertia are suitable for most practical purposes.

It may be shown, when transverse shear effects are neglected in the theoretical procedure, i.e. $\nu \to \infty$, that the theoretical predictions in Sections 3.2.1 and 3.3.1 for a rectangular pressure pulse are identical to the solutions for mechanisms 1 and 2A when $\alpha = 1$ (uniform rectangular pressure pulse) in Florence (1977).

5. CONCLUSIONS

A theoretical solution has been obtained for the dynamic response of a fully clamped circular plate made from rigid, perfectly plastic material and subjected to a large blast pressure loading. An extended Johansen yield criterion is used in the analysis in order to explore the influence of the transverse shear force as well as bending moments on plastic yielding. It is shown that relationships exist between the theoretical solutions for simply supported and fully clamped circular plates, which are similar to the observations made for beams in Li and Jones (1991a).

The boundary conditions exercise a significant influence on the dynamic plastic response of a circular plate. A fully clamped circular plate resists bending deformations more effectively than a simply supported circular plate, though its resistance to transverse shear sliding is inferior.

It is demonstrated that the correlation parameters proposed by Youngdahl (1970) also may be used to eliminate important loading pulse shape effects when the transverse shear force is retained in the yield criterion.

Transverse shear failures (mode III failures) may occur in some situations according to the theoretical analysis presented in this paper and have been observed in some recent experimental tests [see e.g. Teeling-Smith and Nurick (1991) and Nurick and Teeling-Smith (1992)]. The critical conditions for a transverse shear failure are predicted with formulae which are simplified by introducing two loading parameters to characterise any pulse loading shape having a peak value at $t = 0$ and $\dot{p}(t) \leqslant 0$ for $t \geqslant 0$.

It is also shown that the predictions of the bound theorems provide good estimates of the theoretical results, with the lower bound method being particularly accurate.

Acknowledgements—Q. M. Li wishes to express his thanks to Taiyuan University of Technology, The People's Republic of China, for a leave of absence and partial financial support, and to the Impact Research Centre, Department of Mechanical Engineering, The University of Liverpool, for providing research facilities.

REFERENCES

Florence, A. L. (1966a). Clamped circular rigid-plastic plates under blast loading. *ASME J. Appl. Mech.* **33,** 256–260.

Florence, A. L. (1966b). Clamped circular rigid-plastic plates under central blast loading. *Int. J. Solids Structures* **2,** 319–335.

Florence, A. L. (1977). Response of circular plates to central pulse loading. *Int. J. Solids Structures* **13,** 1091–1102.

Hopkins, H. G. (1957). Some remarks concerning the dependence of plastic plate problems upon the yield condition. In *Proc. 9th Int. Cong. Appl. Mech.* **6,** 448–457. Brussels.

Hopkins, H. G. and Prager, W. (1953). The load carrying capacities of circular plates. *J. Mech. Phys. Solids* **2,** 1–13.

Jones, N. (1976). Plastic failure of ductile beams loaded dynamically. *Trans. ASME J. Engng Ind.* **98**(B), 131–136.

Jones, N. (1985). Bounds on the dynamic plastic behaviour of structures including transverse shear effects. *Int. J. Impact Engng* **3,** 273–291.

Jones, N. (1989). *Structural Impact.* Cambridge University Press, Cambridge.

Jones, N. and Gomes de Oliveira, J. (1980). Dynamic plastic response of circular plates with transverse shear and rotatory inertia. *ASME J. Appl. Mech.* **47,** 27–34.

Jouri, W. S. and Jones, N. (1988). The impact behaviour of aluminium alloy and mild steel double-shear specimens. *Int. J. Mech. Sci.* **30,** 153–172.

Kumar, A. and Krishna Reddy, A. A. (1986). Dynamic plastic response of circular plates with transverse shear. *ASME J. Appl. Mech.* **53,** 952–953.

Li, Q. M. and Huang, Y. G. (1989). Dynamic plastic response of thin circular plates with transverse shear and rotatory inertia subjected to rectangular pulse loading. *Int. J. Impact Engng* **8,** 219–228.

Li, Q. M. and Huang, Y. G. (1990). Dynamic plastic response of circular plates with transverse shear. *ASME J. Appl. Mech.* **57,** 1077–1078.

Li, Q. M. and Jones, N. (1991a). Blast loading of fully clamped beams with transverse shear effects. *Impact Research Centre Report* No. ES/78/91. Department of Mechanical Engineering, University of Liverpool.

Li, Q. M. and Jones, N. (1991b). Blast loading of fully clamped circular plates with transverse shear effects. *Impact Research Centre Report* No. ES/79/91. Department of Mechanical Engineering, University of Liverpool.

Martin, J. B. (1964). Impulsive loading theorems for rigid-plastic continua. *ASCE J. Engng Mech. Div.* **90**(EM5), 27–42.

Morales, W. J. and Nevill, G. E. (1970). Lower bounds on deformations of dynamically loaded rigid-plastic continua. *AIAA J.* **8,** 2043–2046.

Nonaka, T. (1977) Shear and bending response of a rigid-plastic beam to blast-type loading. *Ingenieur-Archiv.* **46,** 35–52.

Nurick, G. N. and Teeling-Smith, R. G. (1992). Predicting the onset of necking and hence rupture of thin plates loaded impulsively—an experimental view. In *Proc. of the 2nd Int. Conf. for Structures under Shock and Impact* (Edited by P. S. Bulson), pp. 431–445. Computational Mechanics Publications, Southampton and Thomas Telford, London.

Sawczuk, A. and Duszek, M. (1963). A note on the interaction of shear and bending in plastic plates. *Arch. Mech. Stosow.* **15,** 411–426.

Teeling-Smith, R. G. and Nurick, G. N. (1991). The deformation and tearing of thin circular plates subjected to impulsive loads. *Int. J. Impact Engng* **11,** 77–91.

Wang, A. J. and Hopkins, H. G. (1954). On the plastic deformation of built-in circular plates under impulsive load. *J. Mech. Phys. Solids* **3,** 22–37.

Youngdahl, C. K. (1970). Correlation parameters for eliminating the effect of pulse shape on dynamic plastic deformation. *ASME J. Appl. Mech.* **37,** 744–752.

Youngdahl, C. K. (1971). Influence of pulse shape on the final plastic deformation of a circular plate. *Int. J. Solids Structures* **7,** 1127–1141.